Supersonic Missile Aerodynamic and Performance Relationships for Long-Range Mission Profiles

Robert J. Krieger*
McDonnell Douglas Astronautics Company, St. Louis, Missouri

Closed-form analytical relationships are developed between supersonic missile aerodynamic characteristics such as lift, zero-lift drag, and drag due to lift and performance parameters such as range, velocity, specific range, flight-path angle, and maneuver load factor. These relationships apply to flight profiles for long-range cruise and glide missions. The analytical relationships are developed for climb, cruise, glide, dive, and run-in segments. The results include equations for use in closed-form performance estimates and guiding configuration development.

Nomenclature

C_d = $(1/C_{D_0})(\partial C_{D_0}/\partial V)$
C_D = drag coefficient
C_{D_0} = drag coefficient at zero lift
$C_{D_{00}}$ = reference C_{D_0}
C_L = lift coefficient
C_{L_n} = C_L at load factor n and V_0
C_{L_1} = C_L at load factor 1 and V_0
C_I = integration term
D = drag
D_1, D_2, D_3 = denominator terms
DOF = degree of freedom
dR/dW = specific range
dR/dW_0 = optimum specific range with constant properties
E/W = specific energy
g = gravitational constant
h = altitude
K = induced drag factor
K_d = $(1/K)(\partial K/\partial V)$
K_0 = reference K
L = lift
N_1 = numerator term
n = aerodynamic load factor
n_d = $(1/n^2)(\partial n^2/\partial V)$
P_S = specific excess power parameter
q = dynamic pressure
R = range
R_G = distance for one maneuver cycle
R_o = offset range
R_σ = turn radius
S = reference area
S_d = $(1/SFC)(\partial SFC/\partial V)$
S' = distance along flight path
SFC = specific fuel consumption
SFC_0 = reference SFC
T = thrust
V = velocity
V_0 = optimum velocity with constant properties
V_{ref} = reference velocity
V_I = initial velocity
W = weight
β = atmospheric density gradient divided by density
γ = flight-path angle
γ_I = initial flight-path angle
$\Delta dR/dW$ = change in dR/dW due to variable properties
ΔV = change in V due to variable properties
θ = $V^2\beta/g$
ρ = atmospheric density
ρ_I = initial density
σ = heading angle
ϕ = bank angle

Superscript

$(\dot{})$ = derivative with time

Introduction

THIS paper develops closed-form analytical relationships between missile aerodynamic characteristics (such as lift, zero-lift drag, and drag due to lift) and performance parameters (such as range, velocity, specific range, flight-path angle, and maneuver load factor). The air-to-ground mission profiles considered are LO-HI-LO and boost glide. The analytical relationships are developed for each segment of the above missions; for example, the climb, cruise, dive, and run-in of the LO-HI-LO mission and the climb and glide of the boost-glide mission.

Analytical expressions which relate aerodynamic characteristics to performance parameters have traditionally been developed assuming constant aerodynamic and propulsion characteristics. Classical solutions for level flight, glide, climb, or turn are documented in many sources.[1-3] For nonconstant characteristics, solutions are often developed for small segments of the trajectory over which parameters are assumed constant.[4] Recent results have considered the effect of variable density on glide profiles.[5] Optimized climb solutions using a specific energy approach[6] also have been developed and analytical results have been obtained for variable aerodynamic and propulsion characteristics.[7] The present results use a similar approach to develop maneuvering cruise and long-range glide solutions for optimum velocity. Solutions for constant aerodynamics are developed for the dive and rocket-powered climb.

The missions are described in the following text and the aerodynamic/performance relations applicable to each mission segment developed.

Presented as Paper 82-1289 at the AIAA 9th Atmospheric Flight Mechanics Conference, San Diego, Calif., Aug. 9-11, 1982; submitted Aug. 10, 1982; revision received June 1, 1983.

*Principal Technical Specialist, Aerodynamics Technology. Associate Fellow AIAA.

LO-HI-LO Mission

Figure 1 is a sketch of a typical air-to-ground mission profile. It is performed by a ramjet-powered missile which 1) climbs to its optimum cruise altitude, 2) cruises until it nears the target, 3) dives to a low altitude, and 4) runs in on the designated target. During the cruise and run-in, maneuvers may be required. The high-altitude maneuvers are modeled as high turn-radius cross-range maneuvers. The low-altitude maneuvers are high-g maneuvers. These maneuvers reduce total mission range capability. A solution for segment 1, the minimum fuel climb, with variable aerodynamics and propulsion is available.[7] Solutions for the other three mission segments are described below.

Maximum Range Cruise with Cross-Range Meneuvers

During high-altitude cruise, midcourse threats can be avoided by flying beyond their defended perimeter. The offset distance, R_0, required to avoid intercept is a function of signature, speed, and altitude. Ideally, the cross-range maneuver to avoid intercepts can be approximated by the constant-radius turn, constant-altitude flight path shown in Fig. 2. During this maneuver a greater distance S' is traveled than the downrange distance R_G and a load factor n is required to achieve the turn radius, R_σ. Specific range is reduced relative to the nonmaneuvering case for two reasons. First, the increased load factor increases drag. Second, the downrange distance traveled is only a fraction of the total distance traversed during the maneuver.

To determine the optimum velocity to maximize the downrange distance traveled per weight of fuel, the load factor and a correction for the downrange distance traveled during the cross-range maneuver are required. From the circular arc geometry of Fig. 2,

$$\cos\sigma = \frac{1 - 4R_0^2/R_G^2}{1 + 4R_0^2/R_G^2} \tag{1}$$

$$R_\sigma = \frac{R_0}{2(1-\cos\sigma)} \tag{2}$$

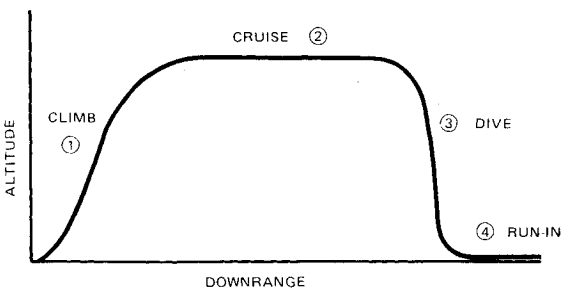

① MINIMUM FUEL CLIMB TO OPTIMUM CRUISE VELOCITY
② OPTIMUM CRUISE WITH CONSTANT RADIUS TURN MANEUVERS
③ THROTTLED, MINIMUM RANGE DIVE TO OPTIMUM RUN-IN VELOCITY
④ RUN-IN WITH HIGH-G MANEUVERS

Fig. 1 LO-HI-LO mission profile.

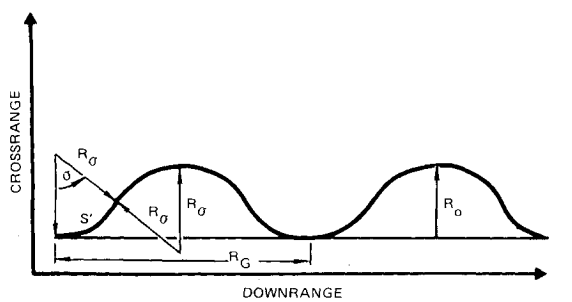

Fig. 2 Flight-path model for constant radius turns.

and

$$\frac{R_G}{S'} = \frac{\sin\sigma}{\sigma} \tag{3}$$

Assuming level flight and neglecting the thrust component of load factor, the vertical component of aerodynamic load factor is 1 and the horizontal component is given by $V^2/R_\sigma g$ where R_σ is given by Eq. (2). The total aerodynamic load factor is given by the vector sum of the two components, i.e.,

$$n^2 = \frac{V^4}{R_\sigma^2 g^2} + 1 \tag{4}$$

The distance traveled downrange per weight of fuel used is

$$\frac{dR}{dW} = \frac{V}{\text{SFC}\cdot D}\left(\frac{R_G}{S'}\right) \tag{5}$$

where thrust is assumed equal to drag to give

$$\dot{W} = \text{SFC}\cdot T = \text{SFC}\cdot D \tag{6}$$

The factor $V/\text{SFC}\cdot D$ is a measure of the total distance traveled per weight of fuel used. However, the useful range is only the downrange component. R_G/S', which is given by Eq. (3), is the ratio of downrange to total distance traveled and corrects specific range.

In Eq. (5), the drag is assumed given by the parabolic form,

$$D = qS(C_{D_0} + KC_L^2) \tag{7}$$

where

$$C_L = nW/qS \tag{8}$$

and the lift coefficient at minimum drag is assumed negligible.

To determine the velocity for optimum specific range at a given R_0 and R_G, Eqs. (3), (4), (7), and (8) can be substituted into Eq. (5) and the result differentiated with respect to velocity and set equal to zero. In the general case, K, C_{D_0}, and SFC are functions of velocity. If weight change with time is assumed small, the final equation has the following form:

$$V^4 = \frac{4K}{\rho^2 C_{D_0}}\left(\frac{nW}{S}\right)^2 \frac{[-(1/V) - S_d - K_d + (4/n^2 V)]}{1/V + S_d + C_d} \tag{9}$$

Both sides of this equation contain the unknown optimum velocity and, therefore, must be solved iteratively. Once V is obtained Eq. (5) is evaluated for the optimum specific range. Although weight change during cruise can exceed 30%, an average weight can be used in Eq. (9) to provide an accurate estimate of average cruise velocity.

If C_{D_0}, K, and SFC are constant, Eq. (9) reduces to the form

$$V^4 = \frac{12K}{C_{D_0}\rho^2}\left(\frac{W}{S}\right)^2 \Big/ \left[1 + \frac{4K}{\rho^2 C_{D_0}}\left(\frac{W}{S}\right)^2 \Big/ R_\sigma^2 g^2\right] \tag{10}$$

As $R_\sigma \to \infty$, the flight path approaches a straight line. At this limit Eq. (10) reduces to

$$C_L^2 = \frac{C_{D_0}}{3K} \tag{11}$$

This is the classical solution[1] for the optimum lift coefficient for maximum specific range at a constant heading.

Equation (9) can be solved by successive approximations. Assume an initial velocity, evaluate the right-hand side of Eq. (9). This result raised to the one-quarter power and the guess are used in a linear iteration scheme which converges in less

Table 1 Example cases

Case	S_d	C_d, $(\text{m/s})^{-1}$	K_d
1	0	0	0
2	4.9×10^{-4}	0	0
3	4.9×10^{-4}	4.9×10^{-4}	4.9×10^{-4}

$R_G = 556$ km
$h = 27.5$ km
$W/S = 1440$ N/m^2
$S = 6.5$ m^2
$K_0 = 1.2$
$C_{D_{00}} = 0.008$
$\text{SFC}_0 = 0.0007$/s
$V_0 = V_{\text{ref}} = 1020$ m/s

than 10 iterations. This procedure was used to evaluate Eq. (9) for three cases in Table 1.

The magnitudes of these derivatives were selected to be typical for a variety of high-performance missile shapes.[7]

Figure 3 compares the velocity and specific range divided by R_G/S' from Eqs. (9) and (5) with 3-DOF numerical results. The 3-DOF were obtained by integrating the equations of motion numerically at a variety of velocities. This results in the curve shown. Equations (9) and (5) predict the numerically determined optimum precisely.

Figures 4 and 5 present optimum Mach number and specific range divided by R_G/S' results obtained from solutions of Eqs. (9) and (5) for the three cases of Table 1 as a function of offset range.

As offset range increases, turn radius decreases. If velocity was held constant, an increased load factor from Eq. (4) would be required to maintain the turn. However, this results in higher C_L and higher drag. The optimization results indicate that a somewhat reduced speed coupled with a slightly increased load factor is a more efficient turn procedure.

Case 2 adds an SFC varying with velocity and shows a reduced optimum Mach number with increased offset range. Reduced Mach number at each offset range is indicated to take advantage of an SFC that is decreasing with lower velocity. For case 3 all parameters vary with velocity. C_{D_0} decreases and K increases with velocity. The resulting optimum Mach number is in between cases 1 and 2. As Fig. 5 shows, in all cases the optimum specific range decreases with increasing offset range.

To reduce the computations required to solve Eq. (9), a first-order perturbation solution of Eqs. (9) and (5) was obtained. Assume that the zeroth-order solution is known for the case of constant SFC, C_{D_0}, and K. Then expand each of the velocity-dependent parameters about this solution, i.e.,

$$V = V_0 + \Delta V \tag{12}$$

$$\text{SFC} = \text{SFC}_0 + \frac{\partial \text{SFC}}{\partial V}\Delta V \tag{13}$$

$$K = K_0 + \frac{\partial K}{\partial V}\Delta V \tag{14}$$

$$C_{D_0} = C_{D_{00}} + \frac{\partial C_{D_0}}{\partial V}\Delta V \tag{15}$$

Also, assume that the logarithmic derivatives, S_d, K_d, and C_d are approximately constant over the speeds of interest. By substituting Eqs. (12-15) into Eq. (9), expanding, neglecting terms of the order $(\Delta V/V_0)^2$ or higher and rearranging, a first-order solution for the optimum velocity change relative to constant C_{D_0}, K, and SFC results in the following:

$$\Delta V = \left[\left(\frac{4K_0C_{Ln}^2}{C_{D_{00}}}\right)(-S_d - K_d) - C_d + K_d\right]\Big/ D_1 \tag{16}$$

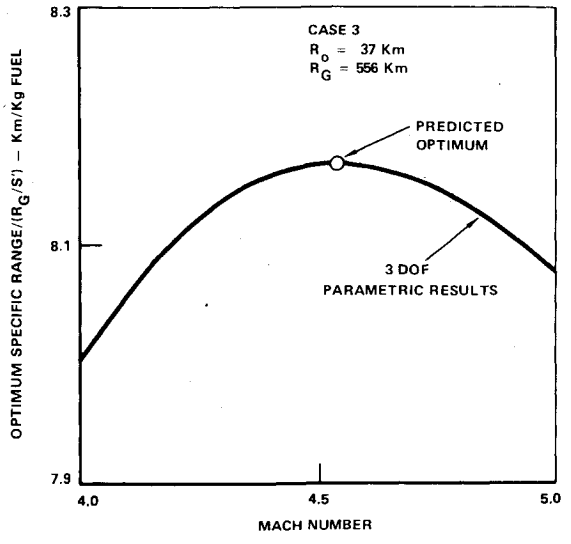

Fig. 3 Comparison of 3-DOF and analytical constant radius turn results.

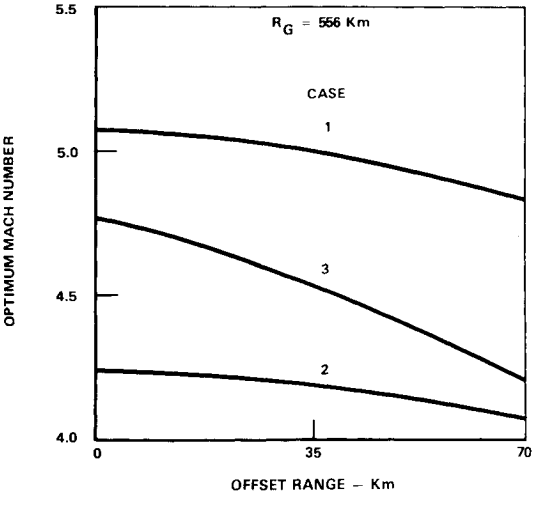

Fig. 4 Optimum Mach number for high-altitude cases.

where

$$D_1 = \frac{4K_0C_{Ln}^2}{C_{D_{00}}}\left[\frac{3}{V_0^2} + \frac{3S_d}{V_0} + K_d\left(\frac{3}{V_0} + S_d + K_d\right)\right] + C_d\left(\frac{5}{V_0} + S_d + C_d\right) - K_d\left(\frac{5}{V_0} + S_d + K_d\right)$$

A similar expansion for specific range, Eq. (5), yields:

$$\Delta\frac{dR}{dW} = N_1\Big/\left(1 + \frac{K_0C_{Ln}^2}{C_{D_{00}}}\right) \tag{17}$$

where

$$N_1 = -\left(\frac{dR}{dW}\right)_0\left[\frac{1}{V_0} + S_d + C_d - \left(\frac{4K_0C_{L1}^2}{C_{D_{00}}}\right)\frac{1}{V_0} + \left(\frac{K_0C_{Ln}^2}{C_{D_{00}}}\right)\left(\frac{1}{V_0} + S_d + K_d\right)\right]\Delta V$$

Equations (16) and (17) are used by first obtaining a solution for constant properties. Pick $C_{D_{00}}$, K_0, and SFC_0

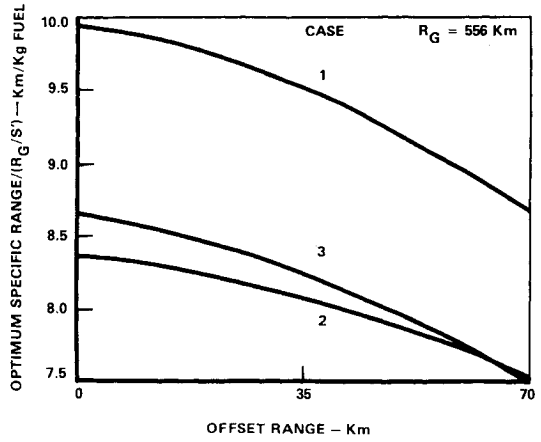

Fig. 5 Optimum specific range for high-altitude cases.

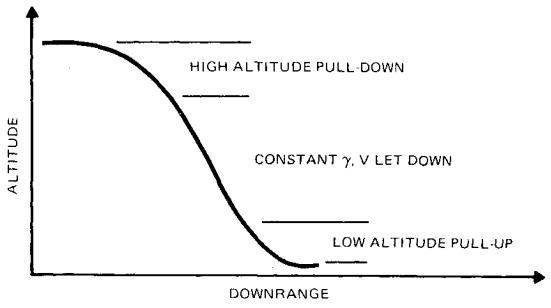

Fig. 6 Flight-path model for the dive.

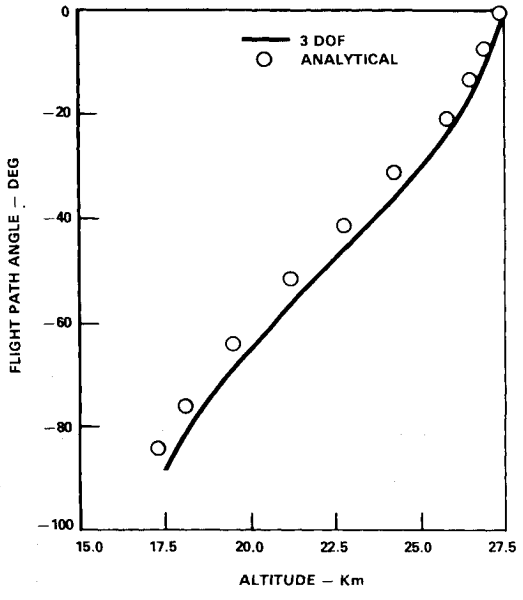

Fig. 7 Comparison of flight-path angle predictions.

which reflect average values within the velocity range of interest. Compute V_0 from Eq. (10), C_{L_n} from Eq. (8), and specific range, dR/dW_0, from Eq. (5). Determine C_d, K_d, and S_d from the slope vs velocity at the average values of C_{D_0}, K, and SFC. Then evaluate Eqs. (16) and (17). The optimum velocity is given by Eq. (12) and optimum specific range by

$$\frac{dR}{dW} = \frac{dR}{dW_0} + \Delta\frac{dR}{dW} \tag{18}$$

Numerical results for ΔV and $\Delta dR/dW$ are usually accurate within 3-10% of the iterative solution for typical cases.

Minimum Range Dive

When the missile nears the target a minimum range dive is desirable before beginning the low-level run-in. Figure 6 shows a simplified flight path for this dive. A pull-down from the cruise condition is assumed achieved at a high C_L. A constant velocity and flight path is flown until the pull-up to low-level run-in. This pull-up is done at a lower C_L because of structural-g limitations. The ideal dive is done with the engine throttled and the resulting velocity at the end of pull-up equal to the optimum run-in velocity. The equations of motion[8] for the pull-down and pull-up were simplified with the following assumptions:

$$T \ll D \tag{19}$$

$$T \ll L \tag{20}$$

$$|\sin\gamma| \ll D/W \tag{21}$$

$$\cos\gamma \ll L/W \tag{22}$$

The equations imply that the lift and drag required to do the maneuver are large, and that the drag and lift divided by weight are much greater than 1.

With these assumptions, the equations of motion reduce to the following:

$$\dot{V} = g(-D/W) \tag{23}$$

$$\dot{\gamma} = \frac{g}{V}(L/W\cos\phi) \tag{24}$$

$$\dot{h} = V\sin\gamma \tag{25}$$

$$\dot{R} = V\cos\gamma \tag{26}$$

Assuming an exponential density variation with altitude, and C_{d_0}, K, and W constant, Eqs. (23-26) can be integrated for the pull-down and pull-up trajectory segments to obtain:

$$\cos\gamma = \cos\gamma_I - \frac{gC_L\cos\phi(\rho-\rho_I)}{2(W/S)\beta} \tag{27}$$

$$V/V_I = \exp\left[\frac{C_D}{C_L\cos\phi}(\gamma_I - \gamma)\right] \tag{28}$$

$$R = \frac{-1}{\beta}\left\{\frac{C_I}{\sqrt{C_I^2-1}}\left[\sin^{-1}\left(\frac{1-C_I\cos\gamma}{C_I-\cos\gamma}\right)\right.\right.$$
$$\left.\left. -\sin^{-1}\left(\frac{1-C_I\cos\gamma_I}{C_I-\cos\gamma_I}\right)\right] + \gamma - \gamma_I\right\} \tag{29}$$

where

$$C_I = \cos\gamma_I + \tfrac{1}{2}g\rho_I C_L\cos\phi/[(W/S)\beta]$$

For the constant γ, V let down the $\dot{V}$ and $\dot{\gamma}$ equations of motion reduce to

$$(-D/W - \sin\gamma) = 0 \tag{30}$$

$$(L/W\cos\phi - \cos\gamma) = 0 \tag{31}$$

which can be solved for γ to give

$$\tan\gamma = -\frac{1}{L\cos\phi/D} \tag{32}$$

and from Eqs. (25) and (26)

$$\frac{dR}{dh} = 1/\tan\gamma \tag{33}$$

The constant γ required to obtain the desired velocity change from high to low altitude is easily computed using Eq. (28) for the velocity. The high- and low-altitude solutions are equated and solved for the velocity and flight-path angle during the constant γ, V let down. Equations (29) and (33) can then be used to define total range. Figure 7 compares a 3-DOF trajectory solution with the results of Eq. (27). Flight-path angle is accurately predicted until nearly 90 deg. Similar accuracy is achieved for velocity and range.

Maximum Range Run-in

To avoid intercept during the low-level run-in, high-g maneuvers are required. The derivation of solutions for this case is similar to that of high-altitude cruise. However, at low altitudes the downrange and range along the flight path are approximately the same. Therefore the S'/R_G correction in Eq. (5) is unnecessary, i.e.,

$$\frac{dR}{dW} = \frac{V}{\text{SFC}\cdot D} \tag{34}$$

In addition, the aerodynamic load factor n is constant and not a function of velocity, as was the case in Eq. (4). The optimum velocity expression for this case becomes

$$V^4 = \frac{4K}{\rho^2 C_{D_0}}\left(\frac{nW}{S}\right)^2 \left\{\left[\frac{3}{V} - S_d - K_d\right]\Big/\left[\frac{1}{V} + S_d + C_d\right]\right\} \tag{35}$$

In the limit of constant properties, Eq. (35) reduces to the classical results of Eq. (11).

As was the case at high altitude, Eq. (35) is solved iteratively. Results are presented for the cases 1, 2, and 3 of Table 1 but at sea level. The cases are renumbered 4, 5, 6, respectively. Figure 8 compares the optimum predicted Mach number and specific range from Eqs. (35) and (34) with 3-DOF numerical results. The optimum is accurately predicted.

Figure 9 presents the Mach number obtained from solutions of Eq. (35) for the three cases as a function of load factor. As load factor increases, C_L increases and drag due to lift increases if velocity is held constant. The results indicate that a higher velocity is desirable to minimize the increased C_L required at higher load factor. Case 5 has a variable SFC. A lower speed is desirable at all Mach numbers to capitalize on the reduction in SFC with lower velocity. Case 6 has all parameters varying and a lower optimum Mach number results. Figure 10 shows the degradation of specific range with increased load factor for all cases. These large load factors are achievable by many supersonic missile designs.

A first-order solution of Eqs. (34) and (35) was obtained analogous to that for high altitude. These results were

$$\Delta V = \left(-\frac{4}{3}S_d - C_d - \frac{K_d}{3}\right)\Big/ D_2 \tag{36}$$

$$D_2 = \frac{4}{V_0^2} + S_d\left(\frac{4}{V_0} + \frac{K_d}{3}\right) + C_d\left(\frac{5}{V_0} + S_d + C_d\right) + K_d\left(-\frac{1}{V_0} + \frac{K_d}{3}\right)$$

$$\Delta\frac{dR}{dW} = -\frac{3}{4}\frac{dR}{dW_0}\left[\frac{4S_d}{3} + C_d + \frac{K_d}{3}\right]\Delta V \tag{37}$$

The accuracy of these equations was evaluated against the exact solution. For representative values of S_d the velocity error was less than 3%.

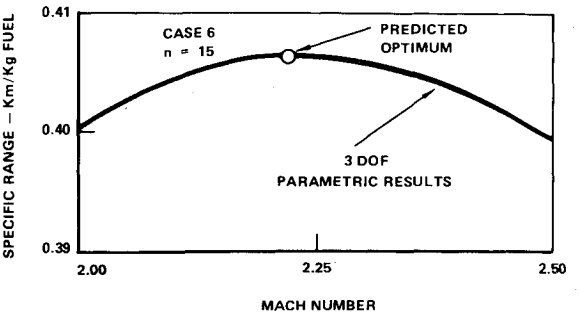

Fig. 8 Comparison of 3-DOF and analytical low-altitude results.

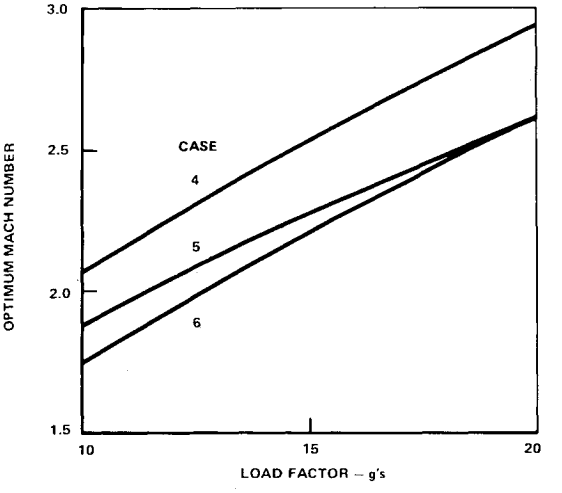

Fig. 9 Optimum Mach number for low-altitude cases.

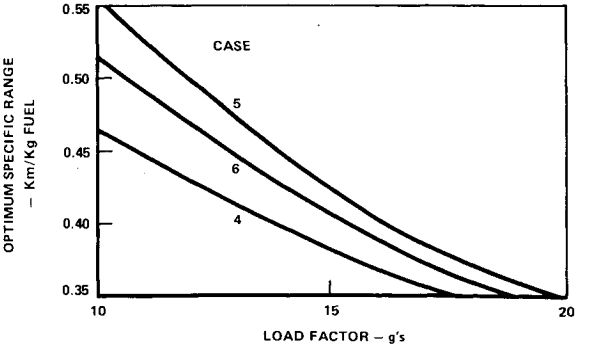

Fig. 10 Optimum specific range for low-altitude cases.

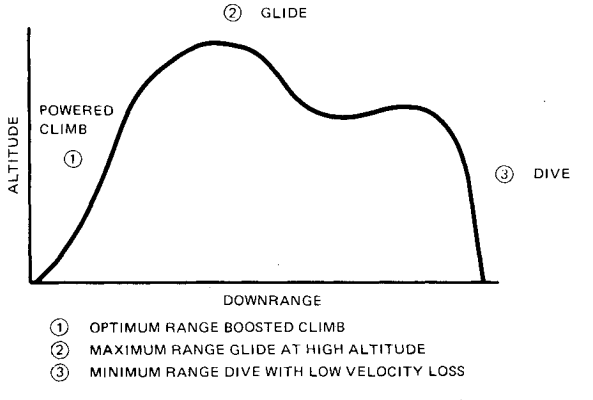

Fig. 11 Boost-glide mission profile.

Equation (36) also can be obtained from Eq. (16). Let $R_o \to \infty$, then $n \to 1$ in Eq. (4) and the zeroth-order solution yields $C_L^2 = C_{d_{0Q}}/3K_0$. Therefore, $4K_0C_{L_n}^2/C_{D_{00}}$ becomes 4/3 in Eq. (16) and it reduces to Eq. (36). A similar substitution in Eq. (17) results in Eq. (37).

Boost-Glide Mission

Figure 11 is a sketch of a typical boost-glide mission profile performed by a rocket-powered missile. The profile is the alternative to a LO-HI-LO mission performed by a ramjet. The dive is the same as for a throttled ramjet. The climb and glide derivations are summarized below.

Rocket-Powered Climb

Maximum energy levels are desired at the end of boost to achieve maximum range. The best climb profile can be established by using a minimum fuel climb derivation,[6] coupled with the equations of motion. The relevant specific excess power parameter and equations of motion are:

$$P_s = \frac{V(T-D)}{W \cdot T \cdot \mathrm{SFC}} \tag{38}$$

$$\dot{V} = g(T/W - D/W - \sin\gamma) \tag{39}$$

If T, W, SFC, C_{D_0}, and K are assumed constant, Eq. (38) can be differentiated with respect to velocity at constant specific energy, E/W. This results in an equation of the form

$$q^2 C_{D_0} S(3-\theta) - q\left[T + 2KS\frac{nW}{S}(2-\theta)\right] + KS\frac{n^2W^2}{S^2}(3-\theta) = 0 \tag{40}$$

$$\theta = V^2\beta/g \tag{41}$$

This equation defines the velocity-density relationship for maximizing energy at climb termination. At low altitudes or high thrust levels, the KS terms are small and Eq. (40) becomes

$$V^2(3-\theta) = 2T/(\rho C_{D_0} S) \tag{42}$$

From Eqs. (39) and (25), $\mathrm{d}V/\mathrm{d}h$ can be defined and equated to the $\mathrm{d}V/\mathrm{d}h$ obtained by differentiating Eq. (42) with respect to altitude. This then can be solved for $\sin\gamma$ to give

$$\sin\gamma = \frac{g/W(qC_dS - T)}{-g + \{\beta TV/[\rho C_{D_0} S(-2V^3\beta/g + 3V)]\}} \tag{43}$$

This is the flight-path angle which gives the optimum climb profile. Figure 12 is a plot of the optimum climb flight-path angle from Eq. (43) as a function of altitude for several thrust-to-weight ratios and case 1 vehicle characteristics. Note that the angle decreases with increasing altitude. For very high T/W, a vertical climbout is indicated.

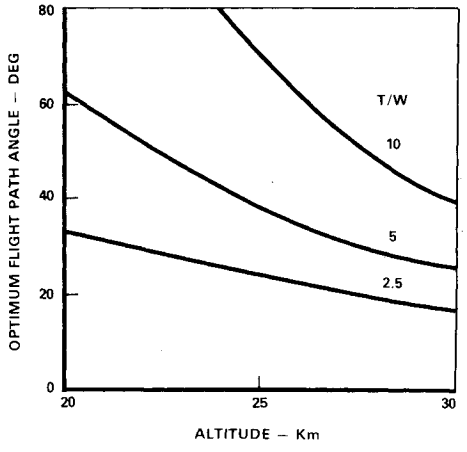

Fig. 12 Optimum rocket-powered climb flight-path angle.

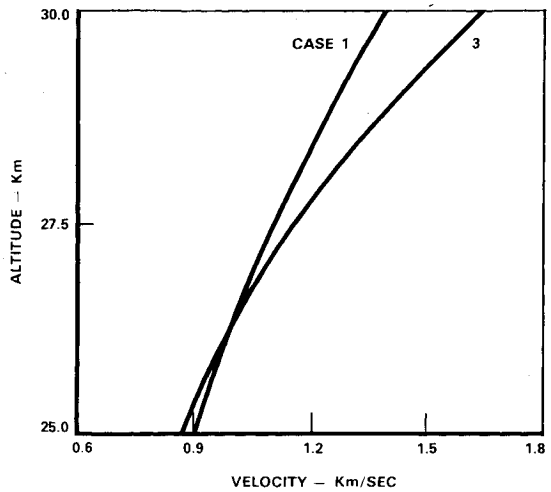

Fig. 13 Optimum glide altitude/velocity comparisons.

Maximum-Range Glide

During the unpowered portion of the flight, the flight path oscillates about the optimum glide path. A solution for the velocity and altitude conditions required to achieve maximum range can be obtained by expressing range in terms of specific energy to obtain

$$R \simeq -\int_{(E/W)_1}^{(E/W)_2} \frac{W\mathrm{d}(E/W)}{D} \tag{44}$$

with the assumption that $\cos\gamma \simeq 1$. Differentiating the integral with respect to velocity at constant E/W gives the following relation.

$$KC_L^2 = C_{D_0}\left[-\frac{V\beta}{g} + \frac{2}{V} + C_d\right] \Big/ \left[-\frac{V\beta}{g} + \frac{2}{V} - K_d - n_d\right] \tag{45}$$

In the limit of constant C_{D_0}, K, and n^2 this reduces to

$$KC_L^2 = C_{D_0} \tag{46}$$

which is the classical solution[2] for the C_L at optimum glide range. Figure 13 compares Eq. (46) results for case 1 with Eq. (45) results for case 3 variable C_{D_0} and K. The high-altitude optimum velocity is larger for case 3 because C_{D_0} is decreasing with increasing velocity.

Equation (45) can be expanded into a first-order solution as done previously for cruise solutions. This results in the expression,

$$\Delta V = \frac{C_d + K_d + n_d}{-D_3}$$

where

$$D_3 = \left(\frac{\beta}{g} - \frac{2}{V_0^2}\right)(K_dV_0 + n_dV_0) + \left(-\frac{\beta}{g} + \frac{6}{V_0^2} + \frac{C_d}{V_0}\right)(C_dV_0) - \frac{4\beta}{g} + \frac{8}{V_0^2} + (K_d + n_d)^2 \tag{47}$$

Summary

Analytical expressions have been obtained for each segment of the LO-HI-LO and boost-glide missions. The expressions can be used for preliminary performance estimates and to identify desirable aerodynamic, propulsion, and design features. All expressions can be evaluated easily on a hand-held programmable computer with total program steps and storage locations less than 1000. For the climb solution, high-altitude cruise, low-altitude cruise and glide, nonconstant aerodynamic and propulsion characteristics can be evaluated.

References

[1]Perkins, C.D. and Hage, R.E., *Airplane Performance Stability and Control,* John Wiley & Sons, Inc., New York, 1967, pp. 155-210.

[2]Miehle, A., *Flight Mechanics, Volume 1, Theory of Flight Paths,* Addison-Wesley Publishing Co., Inc., Reading, Mass., 1962.

[3]Freeman, B., "Simple Analytical Equations for the Velocity of an Airplane in Unaccelerated Level, Climbing and Diving Flight," *Journal of the Aeronautical Sciences,* Vol. 14, March 1947, pp. 185-189.

[4]Jackson, C.M., "Estimation of Flight Performance with Closed-Form Approximations to the Equations of Motion," NASA TR R-228, Jan. 1966.

[5]Raymond, J.L., "Constant L/D Glide Trajectories," AIAA Paper 82-0362, Jan. 1982.

[6]Rutowski, E.S., "Energy Approach to the General Aircraft Performance Problem," *Journal of the Aeronautical Sciences,* Vol. 21, March 1954, pp. 187-195.

[7]Krieger, R.J., "Aerodynamic Design Criteria for Supersonic Climb-Cruise Missiles," *Journal of Spacecraft and Rockets,* Vol. 18, March-April 1981, p. 145.

[8]Miller, L.E. and Koch, P.G., "Aircraft Flight Performance Methods," AFFDL-TR-75-89 (Rev. 1), July 1976.